High-Speed Calorimetry for the Study of the Kinetics of (De)vitrification, Crystallization, and Melting of Macromolecules†

Thijs F. J. Pijpers, Vincent B. F. Mathot,* Bart Goderis, Rolf L. Scherrenberg, and Eric W. van der Vegte

DSM Research, P.O. Box 18, 6160 MD Geleen, The Netherlands

Received June 29, 2001; Revised Manuscript Received October 8, 2001

ABSTRACT: This paper reports on the characteristics and use of a new mode of measurement: High Performance DSC (HPer DSC), which represents a major step forward in high-speed calorimetry, as compared to standard DSC. It facilitates the study of the kinetics and metastability of macromolecular systems, especially the analysis of rate-dependent phenomena in real time. Controlled and constant scan rates at hundreds of degrees per minute and combinations thereof both in cooling and in heating are possible. Heats of transition, heat capacities, temperature-dependent crystallinities, etc. can be established at the extreme rates applied. Examples of the utilization of HPer DSC are given for polymers with respect to the effective hindrance of crystallization and cold crystallization, avoidance of recrystallization and the rate dependency of vitrification and devitrification. Low, milligram-scale sample masses, even down to the microgram level, are utilized. The short measuring times also provide the high throughput needed in combinatorial chemistry.

1. Introduction

In macromolecular and pharmaceutical systems, metastability[1−4] is the rule rather than the exception, and the study of the kinetics of such systems has become an important issue. For a thorough understanding of the kinetics of all kinds of temperature- and time-dependent processes related to metastability, there is an urgent need for new techniques. Keywords are "in situ" and "real time" for techniques capable of analyzing metastable structures on supramolecular scales ranging from "nano" via "meso" to "macro" .

Specifically, a major challenge is coping with realistic conditions as occurring in practice, such as the high cooling rates,[5−9] high pressures,[10−14] and high shear rates[9,15,16] applied in polymer processing,[15,17] which influence vitrification[18] and crystallization[15,19] strongly.

There is likewise a great need for equipment enabling the use of high heating rates[2,5,20−31] Not only is it important to be able to mimic realistic conditions as occurring during a product's life, but also it is crucial to deduce a sample's thermal history using a heating scan. A case in point is the deduction of the glass transition temperature of a sample or product in heating. To avoid enthalpy relaxation (not to be confused with enthalpy recovery), aging, cold crystallization, etc., heating should be as fast as possible.

Another example is the challenge of linking melting behavior to prior crystallization.[19] Quite often, the relationship between melting and crystallization and the resulting morphology is obscured by all kinds of reorganization processes[4,19,29,32] through which the metastable system is striving toward thermodynamic equilibrium during the heating run. Such reorganization can be (partly) avoided by heating at a high rate,[28] so that the relationship between crystallization, the resulting morphology, and subsequent melting becomes transparent. High rates would also be very useful in high throughput projects, as in combinatorial chemistry.

To meet one of the above-mentioned challenges,[29,30] we developed a High Performance DSC (HPer DSC)[33,34] which is a generic name that encompasses quantitative measurement at *very high, controlled (including constant) cooling and heating rates* of hundreds of degrees per minute (high rate DSC) of (sub)milligram amounts of material, thus also facilitating high throughput DSC. Thus, HPer DSC makes high-speed calorimetry possible. Up to now, controlled constant rates as high as hundreds of degrees per minute have been realized, and there is still room for improvement. HPer DSC represents one extreme of the range of possible scan rates, the other extreme being temperature-modulated DSC (TMDSC)[29,35−42] which extended the spectrum to lower rates, including "quasi-isothermal" measurements.

In this communication, a new DSC mode of high-speed calorimetry is presented that will drastically improve researchers' ability to study the kinetics of systems in general, including macromolecular systems, by applying much higher controlled (constant) cooling and heating rates and combinations thereof than were possible up to now. An important aspect of HPer DSC is that it can be used not only for accurately determining the characteristic temperatures associated with a transition but also for quantitatively determining peak areas and in general the entire curve: the new technique yields quantitative results. Heat capacity data are more easily obtained by HPer DSC at extreme scan rates than by standard DSC at conventional rates since instrumental drift is negligible during such rapid measurements. Of course, the time between the experiment with a sample and the experiment without a sample should be kept as short as possible. For (very) high rates to be effective, (very) low sample masses have to be used. The loss of accuracy associated with a sample mass reduction is compensated by the increase in accuracy associated with the application of a higher rate. In fact, the

* Corresponding author. *E-mail address*: vincent.mathot@dsm.com

† (Invited) lectures by V.B.F.M. and M.F.J.P. during the NATAS (North American Thermal Analysis Society) 28th Annual Conference on Thermal Analysis and Applications, October 4−6, Orlando, FL, 2000.

10.1021/ma011122u CCC: $22.00
Published on Web 03/16/2002

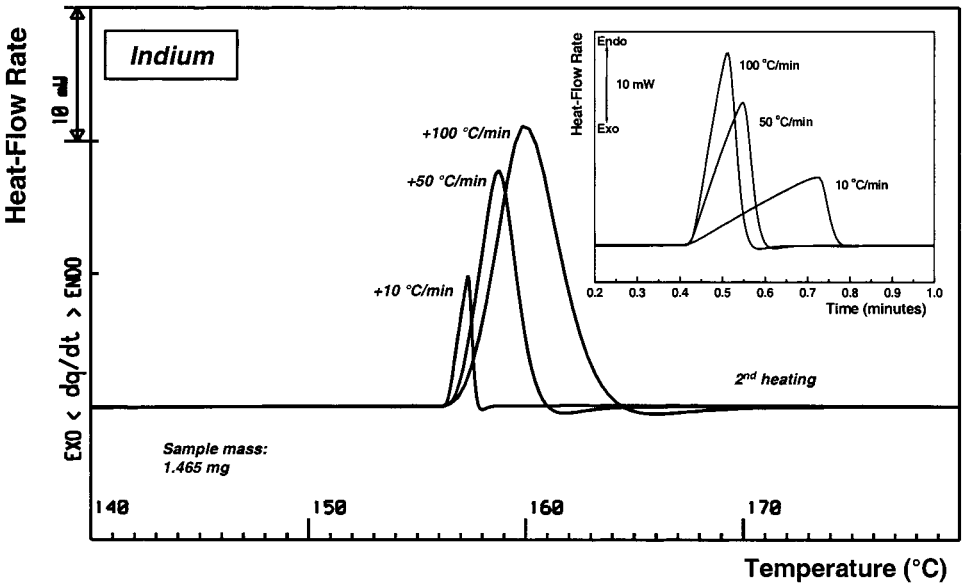

Figure 1. Heating of indium (1.465 mg) at 10, 50, and 100 °C/min after cooling at 10 °C/min. Purge gas: helium (10)/neon (90).

reduction of the sample mass is an additional advantage of the technique as it opens up the possibility to measure samples whose mass is typically in the milligram range or even down to the microgram range. Thus, although the new DSC-mode belongs to the high-speed calorimetry category, the name *High Performance* was chosen deliberately because it involves much more than just a high rate, which in itself is of great interest.

2. Experimental Section

2.1. HPer DSC. General Remarks: Instrumentation and Modifications Made, Calibration, and Sample Handling. Measurements were performed with modified Perkin-Elmer Pyris-1 calorimeters[33] having software versions 3.0 and higher. The reason for selecting this power compensation DSC was that its low furnace mass and small dimensions ensure a much faster heat transfer than in the existing commercial heat-flux DSCs. The small gap between furnace and cooling system (using guard ring inserts) promotes effective cooling. The cryofill system used for cooling represents a very effective heat sink. Special attention was paid to the avoidance of water uptake by the gas tubes in the instrument, to the cooling of the instrument electronics, and to the prevention of water vapor condensation, one of the measures taken being the installation of a glovebox with dry nitrogen purge. The choice of the gas atmosphere (pure gas or a mixture of gases) surrounding the sample containers depends on the specific system and on the temperature range to be studied. In most cases, a mixture of 10% helium and 90% neon is suited for a combination of a temperature range of −176 to 585 °C and typical controlled (linear) scan rates as high as 400 °C/min. Both of these inert gases do not condense under cooling by liquid nitrogen. With regard to the heat conduction around the sample containers, the mixture offers a useful compromise.[43] Pure helium is in itself an excellent heat conductor and can be used to maximize heat transfer, which offers benefits in measurements down to low (subambient) temperatures. However, when it comes to reaching high temperatures, the furnace will be a limiting factor, because the helium causes too much heat to be lost so that the furnace can no longer control the temperature beyond the ceiling level of about 200 °C. Neon[44] conducts heat less well (but better than nitrogen), and makes it possible to control the temperature in the higher ranges. It is even possible to use standard nitrogen as long as it is prevented from condensing as a result of the presence of liquid nitrogen cooling. This is sometimes possible, depending on the route taken by the gas. Default isothermal waiting times between runs amount to 5 min, although this time can be shortened to, e.g., 1 min. To promote optimal thermal contact between the sample and the sensor, a 15-μm thin aluminum foil of approximately 0.5 × 1 cm^2 is normally used to wrap the sample, instead of using a pan as sample container. If a lower accuracy is acceptable, it is also possible to use pans of aluminum, even in combination with a sample exchanger. Low sample masses are used, typically around 1 mg and lower. Temperature calibration is performed and checked with indium, tin, lead, and zinc at 10 °C/min. Power calibrations are performed using indium and checked using indium and Sapphire. A furnace calibration is performed in which the furnace temperature and sample temperature are equaled. Zinc, adamantane, and 4,4-azoxyanisole are used for checking the calibration in cooling vs heating, again at 10 °C/min. This calibration in cooling is not an absolute one: it depends on the calibration in heating. The three substances mentioned are very useful for calibration because they show no supercooling at the transitions used: crystallization ⇔ melting (zinc); solid ⇔ solid (adamantane); anisotropic ⇔ isotropic (4,4-azoxyanisole). After calibration at 10 °C/min, using software versions 3.0 and higher, the Pyris-1 turns out to be accurately calibrated *for all other scan rates*, including the very high ones. Curves are normalized for sample mass and rate. In cases where quantitative measurements are desired, all curves are corrected for any remaining instrumental drift and curvature by subtracting empty foil or pan measurements, as is the normal procedure in heat capacity measurements.[45]

2.2. HPer DSC. Calibration for High Scan Rates, both in Cooling and in Heating. Figure 1 shows how indium melts at different heating rates. The onset of melting is the same for all curves (one and the same indium sample having a mass of 1.465 mg is used throughout), though the slopes on the low-temperature side are different. In Figure 1, the area (in mW °C) under the curves measured (i.e., the area enclosed by the curve measured and the line that connects measuring points at temperatures below and above the transition) increases in proportion to the heating rate. In the case of power compensation DSC, the heat of fusion in joules—which equals the aforementioned area divided by the scan rate—is independent of the heat transfer rate and hence also of the scan rate. It does indeed appear to be constant, provided that the area of any "undershoot" (leading to lower measuring values than those obtained for the melt at temperatures at which melting has virtually been completed, see Figure 1) is taken to be negative. It is possible to arrive at the same curve shape at all rates—and one should strive to do so—if at increasing rates the sample mass is lowered proportionally; see discussion at Figure 4. The inset in Figure 1 shows the corresponding heat flow rate against time curves for the same indium sample.

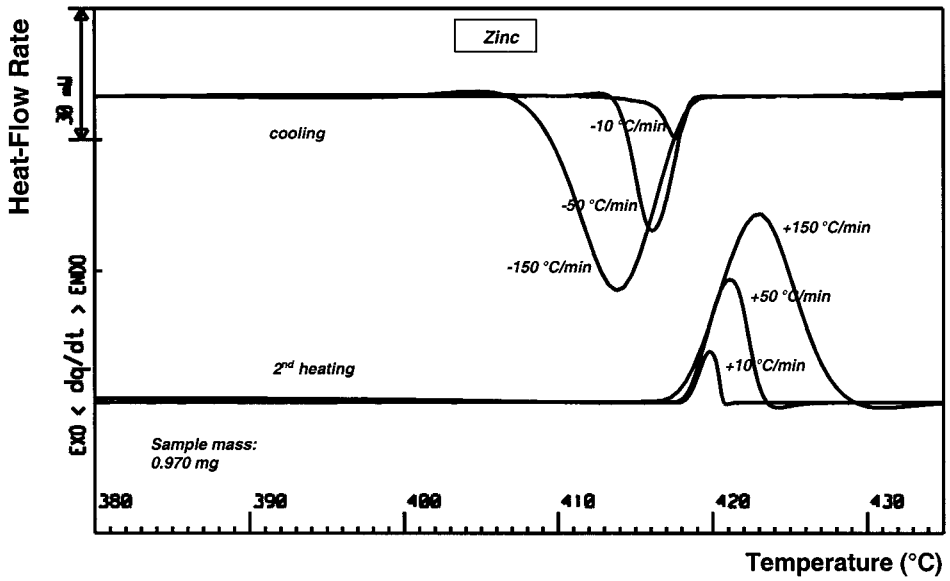

Figure 2. Cooling of zinc (0.970 mg) at 10, 50, and 150 °C/min, and subsequent heating at the same rates respectively. The crystal ⇔ melt transition shows no supercooling. Purge gas: helium (10)/neon (90).

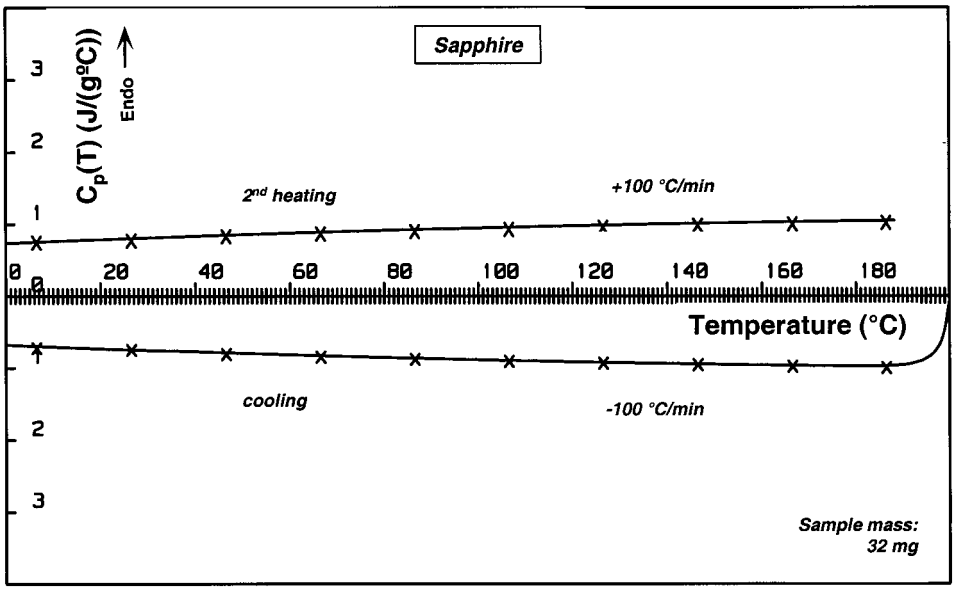

Figure 3. Continuous heat capacity measurements in cooling and subsequent heating of Al2O3 (sapphire, 32 mg disk of circular shape, 6 mm in diameter, in standard pan) at 100 °C/min, and comparison with literature values. Purge gas: helium (10)/neon (90).

Since HPer DSC is used both in *cooling* and in heating, calibration in cooling is at least as important. Figure 2 shows cooling and heating curves for zinc, one of the calibrants that can be used for this purpose. Leaving aside a few subtle differences between the curves, the important observation is that in the case of zinc the extrapolated onsets of crystallization (in a cooling run) and melting (in a heating run) lie at virtually the same temperature, and that this is the case for all rates after calibration at 10 °C/min, see Figure. A similar picture was observed for the solid ⇔ solid transition of adamantane and for the anisotropic ⇔ isotropic transition of 4,4-azoxyanisole. On the basis of experience gained so far, it can be concluded that calibration at high scan rates is straightforward. Thus, it is found that a HPer DSC that has been calibrated according to the standard procedure at a "conventional" scan rate, such as the 10 °C/min applied in the above case, it is, remarkably enough, also accurately calibrated at high rates (this has been checked up to 500 °C/min) in both cooling and heating.

It is a standard procedure to carry out the enthalpy calibration with indium. In that case, it turns out that the PerkinElmer power compensation DSC is accurately enthalpy-calibrated as well over a much wider temperature range than the indium melt transition region. This is shown in Figure 3 on the basis of heat capacity measurements on Al_2O_3 (sapphire) at −100 to +100 °C/min according to the 'continuous measuring method'.[45]

Figures 1 and 2 display peak broadening ("thermal lag") with increasing scan rates. Thermal lag is in fact a general problem, which is always observed when using traditional calorimeters at "conventional" , low scan rates. For instance, indium melts within 0.05 °C[46,47] during stepwise heating while at a moderate rate of 10 °C/min the melting range already amounts to nearly two degrees. Thermal lag depends on numerous factors, such as the capability of the instrument to add energy during heating (or to remove energy during cooling) as fast as possible; the response time of the instrument; the heat conduction from the heater to the pan used and subsequently within the sample and the response from the sample to the sensor. Thermal lag, and in general heat transfer issues relating to DSC instruments,[48,49] have received a great deal of attention recently because they have a strong impact on the

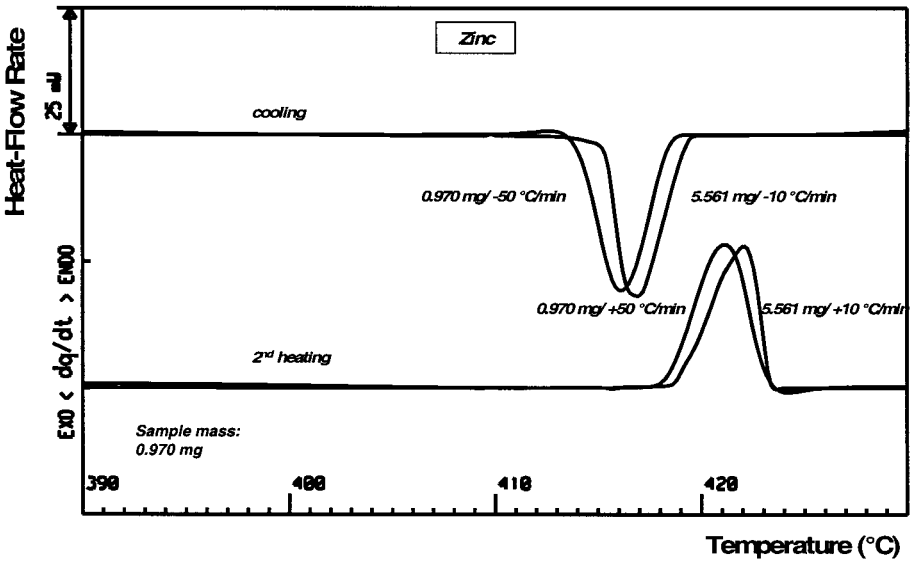

Figure 4. Cooling and subsequent heating of zinc with different combinations of sample mass and scan rate: 0.970 mg at 50 °C/min and 5.561 mg at 10 °C/min, showing the inverse influence sample mass and scan rate have on curve shape. Purge gas: helium (10)/neon (90).

results of TMDSC and indeed temperature-modulated calorimetry in general.[50] However, the issue here is whether, and if so to what extent, the use of extremely high rates results in an *increase in thermal lag beyond values commonly accepted at the moment*. Such an increase can be effectively avoided, as will be demonstrated and explained below.

Any researcher will, on one hand, try to keep the sample mass as low as possible to minimize thermal lag. Obviously, on the other hand, the sample should have a certain minimum mass to ensure a measurable signal and an acceptable signal-to-noise ratio. Moreover, the higher the sample mass, the more accurate the peak area. So, usually, in the case of traditional calorimeters, a compromise has to be found, for example a sample mass of about 5 mg in combination with a scan rate of 10 °C/min. Thus, in the case of high rates as applied in HPer DSC, to maintain a peak shape (i.e., to avoid any additional peak broadening) which is commonly accepted at the moment, the sample mass has to be reduced. This turns out to pose no problem, because in the case of a PerkinElmer power compensation DSC—even under the extreme conditions studied here—the sample mass and scan rate are closely interlinked. It follows that in the case of HPer DSC, too, if the scan rate is increased by a factor of x, the sample mass has to be reduced by the same factor x. Figure 4 shows that this leaves the peak shape unchanged in the case of zinc.

The example in Figure 4 shows that thermal lag does not necessarily increase. This illustrates that the Pyris-1 instrument and its software is capable of effecting an adequate heat transfer under the conditions chosen, and the examples given later on will show that it retains this capability even under more extreme conditions. The following observations in particular illustrate that the calorimeter continues to function well under those conditions:

- Rather than increasing, as one would expect in the case of an increase in thermal lag, the melting temperatures of polymeric samples remain constant or decrease as the scan rate increases.
- At higher cooling rates the glass transition of a polymeric sample shifts to higher temperatures, as one would expect for thermodynamic reasons, rather than to lower temperatures, as one would expect in the case of an increase in thermal lag.
- In the case of recrystallization of a polymeric sample, the intensities of the peaks do change with increasing heating rates, as expected, but the positions of the peaks relative to the temperature axis remain unchanged.
- For 4,4-azoxyanisole, whose thermal conductivity is between that of polymers and metals, the anisotropic ⇔ isotropic transition in heating and cooling remains at the same temperature, even in measurements at +150 and −150 °C/min, respectively, a difference of as much as 300 °C/min.

In our opinion, there is an additional reason for the system's excellent performance besides its demonstrably adequate response in the case of notoriously "difficult" samples such as polymers (difficult in terms of heat transfer), namely the use of aluminum foil instead of a pan as sample container. The aluminum foil has a much lower mass and, more importantly, provides a drastically improved way of heat transfer. Instead of one-dimensional heat transfer (from the aluminum bottom of a pan to the sample), there is now a three-dimensional transfer as it were (from the surrounding aluminum foil to the sample, from all sides). Moreover, since the sample mass can be varied at will, down to microgram level, in our experience there is no *extra* thermal lag compared with measurements at conventional, low scan rates. Therefore, if the aim is to reduce thermal lag—see the observation made with regard to indium—one would do well to improve the performance of traditional thermal analysis equipment under conventional conditions—especially in cases where the DSC is used as TMDSC and especially for polymers, which are notoriously poor heat conductors. Under such conditions, thermal lag deserves to be given more attention than it has received until now, because in many cases samples with high masses and correspondingly large dimensions are chosen which, in combination with a DSC pan, result in downright poor heat transfer in the sample. This will definitely be the case for samples with "difficult" shapes, such as powders. As noted earlier, the problems mentioned for standard DSC have received a great deal more attention, and insight into them has greatly increased, on account of their major impact on the performance of TMDSC. However, no dramatic improvement is to be expected unless improved hardware is developed, see the "Outlook" section. If one were forced to make a choice, the combination of high rate/low sample mass and small dimensions would be preferable to the combination of low rate/high sample mass and large dimensions. In other words: measurements at high rates do not pose any bigger experimental problems than measurements at conventional rates—on the contrary—provided the right precautionary measures are taken.

An obvious question is given as follows: If the scan rate is increased from 10 °C/min to an extreme value, for example 500 °C/min, will a corresponding decrease in sample mass from, e.g., 5 mg to 100 μg present any problem with regard to the measuring signal and the signal-to-noise ratio? The answer is given by Figure 5, which shows the results of a HPer DSC measurement on a ultrahigh molecular weight polyethylene

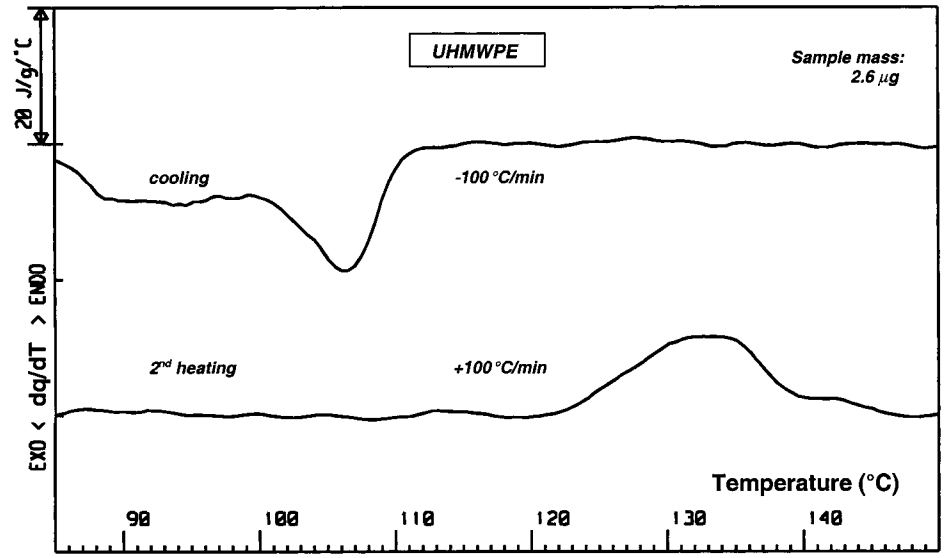

Figure 5. Very high scan rates facilitated by the capability of HPer DSC to perform measurements on minute amounts of substances, in this case 2.6 μg of a ultrahigh molecular weight polyethylene sample. Purge gas: helium (10)/neon (90).

sample with a mass of 2.6 μg, much less than was assumed to be necessary to answer the above question. As Figure 5 shows, measurement of this sample presents no problem. In fact, instead of measuring in a 10 mW range (corresponding to for example a typical peak height of a polymer as measured in standard DSC conditions) we measured under conditions where the peak height lies in the 100 μW range, bridging a factor 100 difference. The unused "margin" of about 40 (2.6 μg compared with 100 μg) may be needed when measurements are performed on a polymer or other material having an intrinsically lower heat of transition.

The ability to measure on a low sample mass—from milligram level down to micrograms—opens the door to quite different applications: just to mention some of the systems brought within reach are coatings and very thin layers, such as in multilayer films,[30] heterogeneities in samples such as gels or additives, tiny amounts as produced in high throughput/combinatorial chemistry, etc. The method also opens up tremendous opportunities for studying the crystallization/melting behavior of fractions[19] obtained by small-scale fractionation methods.[33] Of course, one should be aware that the small dimensions corresponding to low sample masses can influence the crystallization behavior, in particular nucleation, because they have an influence on the number of active nuclei[1,51−56] and/or because they lead to a change in the way nucleation takes place (for example transnucleation becoming the prevailing mode[8,57]). Therefore, it is always a good idea to use other techniques besides DSC, in particular microscopy, to detect any changes. Besides the aluminum foil used here, other foils (such as gold) can of course also be used for special purposes, as long as they have the right heat conductivity.

2.3. HPer DSC. Linearity in the Case of High Scan Rates, both in Cooling and in Heating. An important aspect of HPer DSC is the linearity of the temperature−time relationship during a measurement, in other words the constancy of the scan rate. Most DSCs, including heat-flux DSCs, are capable of heating at reasonably high rates. Of course, DSCs differ in the degree to which the sample temperature—of which the sensor temperature gives an indication—lags behind the program temperature and the furnace temperature. This is because across the entire chain from furnace to sample there are differences in heat transfer due to differences in equipment construction. Cooling at a high rate is much more difficult, and most DSCs are incapable of realizing a constant cooling rate higher than, typically, 20 °C/min. One should strictly adhere to the procedures supplied by the manufacturer (see instrument specifications) because otherwise the measurements will result in blatantly erroneous results, as the reader can easily verify by performing such experiments using existing equipment. Furthermore, the relationship between temperature and time will be anything but linear.

The capabilities of HPer DSC in this field are easy to demonstrate. Figure 6 shows both sensor temperature measured and the program temperature as functions of the linear temperature−time programs imposed. Although the actual sample temperature will intrinsically lag somewhat behind the sensor temperature, this effect is not noticeable, thanks to the temperature calibration procedure applied. Cooling and heating scans were programmed with constant scan rates of 50, 100, and 200 °C/min, over a wide temperature range: from −120 to +500 °C. In every case, the heating scans coincide with each other and the programmed $T-t$ ramps were always realized. It was not investigated to what temperatures above +500 °C this still holds. The results obtained in the cooling scans vary as a function of the cooling rate programmed. In the −50 °C/min scan the result is perfect: the programmed $T-t$ ramp is realized over the entire temperature range. However, at higher cooling rates, the sensor temperature lags behind (i.e., is higher than) the programmed temperature in the low-temperature range. In the −100 °C/min scan, the two temperatures diverge below about −75 °C, and in the −200 °C/min scan, they diverge below about 0 °C. Even so, the objective of achieving high, constant scan rates over wide temperature ranges is amply met: in the −50 °C/min scan the temperature range over which the scan rate is constant spans more than 620 °C, in the −100 °C/min scan it spans about 575 °C and in the −200 °C/min scan it spans about 500 °C. In general, the conditions chosen (in particular the "heat sink" temperature, i.e., the lowest temperature that can be achieved by the cooling system but also the scan rate itself, the measuring range, the composition of the purge gas, etc.) should be such that in the measuring range of interest, where actual processes such as vitrification, (cold) crystallization, melting, or reorganization occur, a constant scan rate is achieved. The choice of a linear relationship between temperature and time is an obvious one because it is simple. But it should be clear that any $T-t$ ramp can be programmed, so that complex situations occurring in practice can be mimicked (at least as far as the scan rate is concerned). Moreover, an analytical $T-t$ relationship makes it easier for other researchers to repeat experiments using different equipment. In high-rate experiments based on DTA and heat-flux DSC there is usually no well-defined $T-t$ relationship, which means these experiments are very hard to duplicate.

Figure 7 gives a detailed overview of how a high scan rate experiment proceeds. This time the scan rates were increased to −300 to +300 °C/min, the temperature range was once again

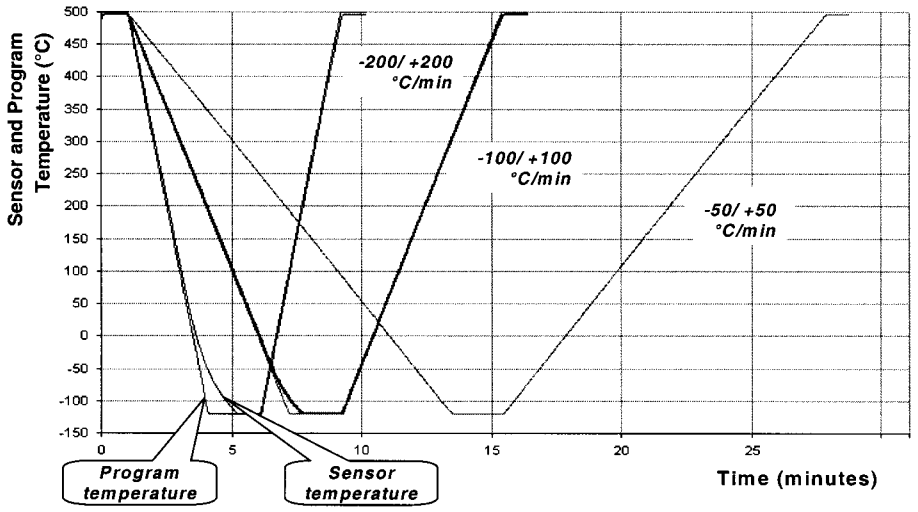

Figure 6. $T-t$ ramps for two empty pans: sensor temperatures recorded and program temperatures chosen against time in the case of cooling and heating rates of 50, 100, and 200 °C/min, in a temperature range of −120 to +500 °C. Purge gas: helium (10)/neon (90).

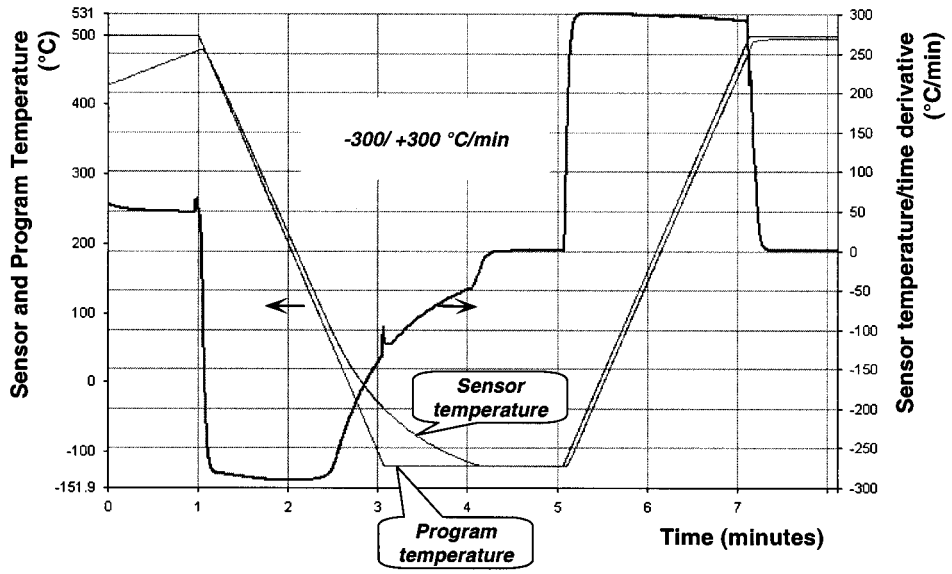

Figure 7. $T-t$ ramp for two empty pans: sensor temperatures recorded and program temperatures chosen against time in the case of cooling and heating rates of 300 °C/min, in a temperature range of −120 to +500 °C. Also shown are the sensor temperature/time derivatives, representing the scan rates realized. Purge gas: helium (10)/neon (90).

from −120 to +500 °C. The figure not only shows the sensor temperature and the program temperature plotted against time but also the sensor temperature/time derivatives. It can easily be seen that in the cooling scan a rate of about −290 °C/min is achieved between 500 and about 75 °C, that is, over a temperature range of about 425 °C. Between +75 and −120 °C the cooling rate decreases to −50 °C/min. In the heating scan, the programmed scan rate of +300 °C/min is achieved across the entire temperature range from −120 to +500 °C. The HPer DSC is capable of achieving even higher scan rates in heating: +500 °C/min is feasible.

In some cases, a smaller temperature range, from −150 to about +200 °C, suffices. This is an interesting measuring range for a number of polymers, in particular polyolefins (including EPDM rubbers). Figure 8 shows the results obtained at scan rates of −100 to +100 °C/min and −200 to +200 °C/min. Again, the two heating scans coincide and the programmed $T-t$ ramps are realized. In the −100 °C/min cooling scan, the result is virtually perfect: the temperature range at which the programmed $T-t$ ramp is realized extends to below −100 °C. In the case of the −200 °C/min scan, this range extends to below −50 °C. For the aforementioned polymers this result is more than satisfactory. It should be noted that in this temperature range pure helium was used as a purge gas in order to maximize heat transfer.

Finally, Figure 9 gives an impression of the lowest temperatures that one can achieve while still maintaining a virtually linear sensor temperature−time relationship, in other words a constant cooling rate, as a function of the programmed cooling rate. As discussed earlier, these lowest temperatures depend on the variables chosen, such as the highest starting temperature (500 °C in Figure 9) and the purge gas used [in Figure 9 this is a helium (10)/neon (90) mixture].

3. Results and Discussion

Two of the target applications of HPer DSC mentioned will now be discussed in more detail: the study of the kinetics of various processes under realistic conditions of measurement and the elucidation of the metastability[3] of the resulting phases.

The time required for the crystallization of long-chain molecules varies, depending on the environment and the experimental conditions, in particular the actual temperature in relation to the equilibrium melt temperature

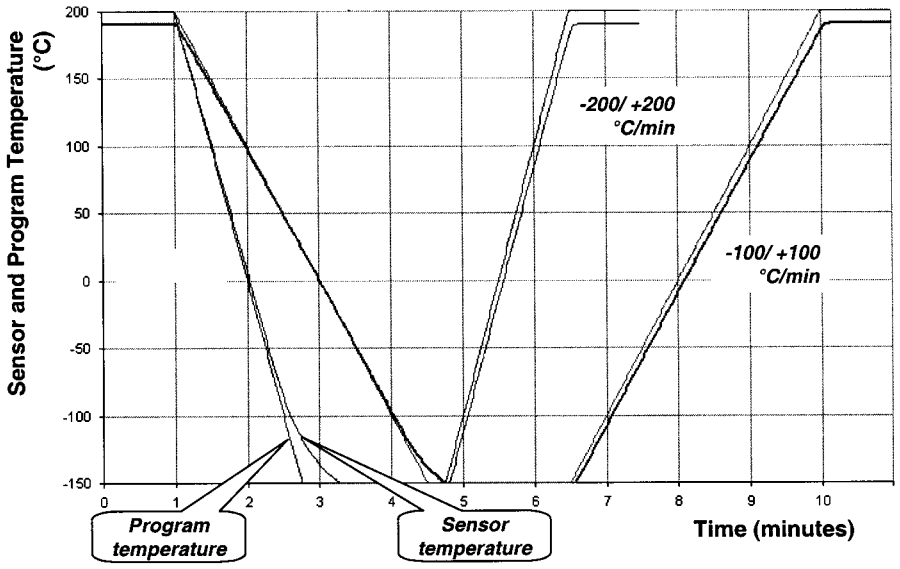

Figure 8. $T-t$ ramps for two empty pans: sensor temperatures recorded and program temperatures chosen against time in the case of cooling and heating rates of 100 and 200 °C/min, in a temperature range of −150 to +200 °C. Purge gas: helium.

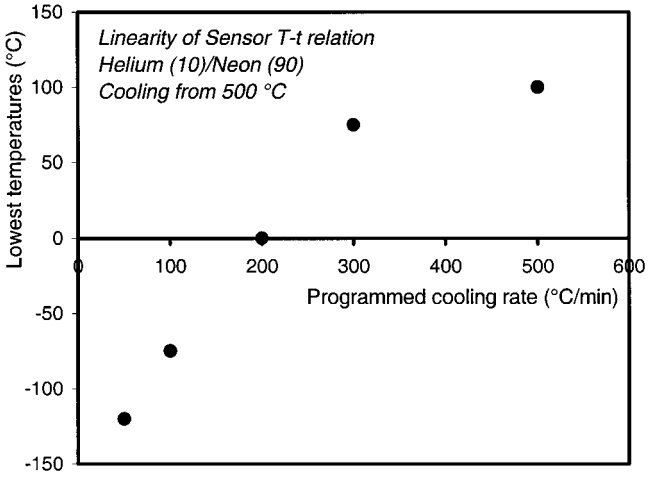

Figure 9. Lowest temperatures that can be achieved while maintaining a virtually linear relationship between the sensor temperature and time (in other words a constant cooling rate), as a function of the programmed cooling rate for two empty pans. Highest starting temperature 500 °C; purge gas consisting of a helium (10)/neon (90) mixture.

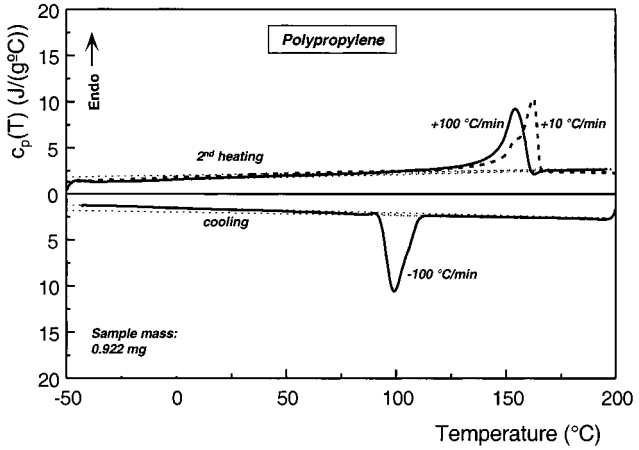

Figure 10. Cooling at 100 °C/min of a polypropylene sample (0.922 mg) giving rise to crystallization at relatively low temperatures (compared to cooling at 10 °C/min). Subsequent heating at 10 °C/min results in a double peaked curve because of melting followed by immediate recrystallization; heating at 100 °C/min, however, results in a single peaked curve because recrystallization is effectively suppressed. Purge gas: helium (10)/neon (90).

and the glass transition temperature.[1,58] The amount of time thus consumed can be in competition with the time available for crystallization. Thus, the development of crystallinity can be reduced by increasing the cooling rate, and it will be minimal at very high cooling rates, such as occur during injection molding. Therefore, to be able to mimic processing conditions and to gain insight into crystallization phenomena as a function of the molecular structure of macromolecules,[19] it is essential that thermal analysis instruments offer the possibility of applying a wide range of cooling rates. This will also make it possible to determine the cooling rate at which the sample does not crystallize at all, and to study the efficiency of nucleants for crystallization.

Another intriguing phenomenon is the fact that quite often melting temperatures as a function of molar mass or cooling rate do not resemble the crystallization temperatures observed during the preceding cooling step.[19,32] This must be caused by extensive reorganization phenomena during heating. Such phenomena can be effectively avoided by cross-linking[29,59,60] or etching away the amorphous phase, but these are complicated and risky routes. For most polymers, measuring at heating rates much higher than the applied cooling rates is a more convenient route to take.

The same applies in the case of recrystallization. Figure 10 presents an example, where a polypropylene (PP) sample heated at 10 °C/min after relatively fast cooling at 100 °C/min shows a melting peak at 163 °C and a shoulder at approximately 155 °C.[33] It is well-known that at such a high cooling rate, and certainly at even higher cooling rates, the main peak is caused by a melting process following the recrystallization of the part melted around 155 °C. So, in fact, the melting at 155 °C is linked directly to the preceding crystallization, in this case around 100 °C. Heating at 100 °C/min shows the real link, because obviously recrystallization is impossible at this high rate. In this way, the interpretation of measurement results is greatly simplified. Another advantage is the possibility of operating and experimenting at high cooling rates. Even the moderate

rate of 100 °C/min lowers the crystallization temperature by approximately 12 deg compared with cooling at 10 °C/min. In the case of PP, high scan rates open up even more possibilities. In PP the occurrence of various crystalline phases, such as α, β, and γ, is to a large extent determined by the $T-t$ ramps imposed on the samples, although the presence of specific nucleating agents also plays a role. Obviously, if an extremely large variation in scan rates in both cooling and heating (and combinations thereof) can be applied, the development of such phases can be influenced very effectively. Also, the kinetics of these processes and any transitions between them can be studied, and compared with evidence obtained by other techniques, such as X-ray analysis.

The measurements at −100 °C/min and +100 °C/min in Figure 10 are quantitative. They are in fact heat capacity measurements according to the "continuous measuring method":[45] the designation "c_p" along the y-axis applies to the measurements at high scan rates. The measurement at +10 °C/min is not quantitative as far as the curve shape is concerned, but it is quantitative with respect to the characteristic peak temperatures. The explanation for the nonquantitative measurement of c_p at +10 °C/min is that a low sample mass (0.922 mg) was used because the high scan rate experiments were to be performed with the same sample. To arrive at a quantitative measurement for the extremely difficult combination of such a low sample mass with the low heating rate of +10 °C/min would necessitate a separate optimization of the apparatus, which was not the aim of this experiment. This highlights an important capability of *High Performance* DSC: it enables heat capacity measurements to be carried out at 100 °C/min! This is a great step forward, the more so as the measurement is no more difficult than a heat capacity measurement at 10 °C/min. On the contrary: the higher rate results in a shorter *overall* measuring time. This minimizes the risk of instrumental drift occurring during the time the sample is measured and during the measurement of an empty aluminum foil (or an empty pan) and thus increases the likelihood of a quantitative result being obtained. However, it has to be emphasized here that heat capacity measurements are never simple,[45] not even with HPer DSC: they are feasible, but only if the instrument is thoroughly optimized and if the experimenter is highly skilled and extremely critical.

Figure 11 illustrates the capability of HPer DSC to influence the nucleation process during crystallization. If the polymer [a poly(ethylene terephthalate) (PET) sample[33]] is cooled at 100 °C/min, it remains amorphous right down to the glass transition, which starts at about 90 °C. Apparently, the rapid cooling process does not allow the sample the time needed for nucleation. The same PET sample partially crystallizes if it is cooled at a lower rate, 10 °C/min.[30,33] If, after cooling at 100 °C/min, the sample is subsequently heated at 10 °C/min, cold crystallization takes place on a large scale immediately after devitrification, with a maximum signal at 160 °C. After that, the melting process starts, with a maximum signal around 250 °C. However, if the sample is heated at a higher rate, 100 °C/min, cold crystallization is virtually prevented. The figure shows that there is still some cold crystallization between the glass transition and about 150 °C and that the material that crystallizes in this range melts again above about 200 °C. So, in conclusion, for this sample, heating at 100 °C/min reduces cold crystallization to virtually zero and the heating curve obtained much better reflects the preceding cooling run—which amorphized the sample. This is of course very important in cases where an "as received" sample has to be analyzed whose thermal history is not known. In such cases it is essential to avoid reorganization in the broadest sense of the term, including cold crystallization and recrystallization, to be able to form an accurate picture of the effects of the sample's thermal history, such as crystallization, annealing, vitrification, aging[18] and the formation of a rigid amorphous phase.[45]

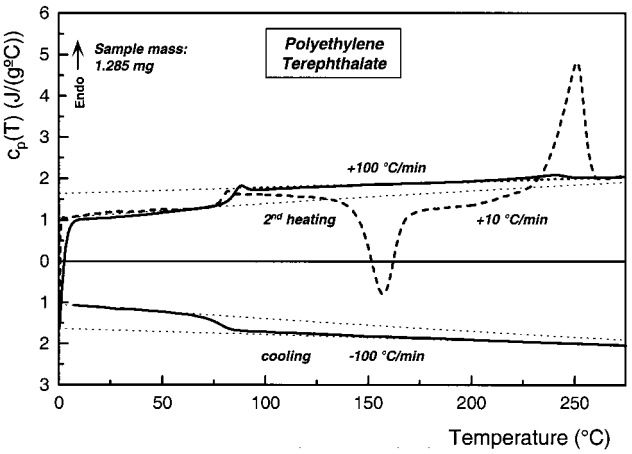

Figure 11. During cooling at 100 °C/min of a polyethylene terephthalate sample (1.285 mg) no crystallization occurs, just vitrification. During heating at 10 °C/min (---), after devitrification, extensive cold crystallization and subsequent melting takes place; heating at 100 °C/min (—) nearly suppresses cold crystallization and subsequent melting. Purge gas: helium (10)/neon (90). The dotted lines represent the reference curves for purely amorphous and purely crystalline PET.

Again, the −100 and +100 °C/min curves are heat capacity curves and are in good agreement with the reference curves for purely amorphous and purely crystalline PET;[61] see the dotted curves. And again, the heating curve measured at 10 °C/min is not a heat capacity curve, because the measurement was not optimized for this combination of a low scan rate and a low sample mass (1.285 mg).

Not all PET samples remain amorphous in a cooling scan at 100 °C/min. In some grades, crystallization can still occur, for instance if the material has a low molar mass, if nucleating agents are added to the samples, etc. Such a sample[33] will be briefly discussed here. On cooling at 10 °C/min this particular PET sample crystallizes around 200 °C, resulting in a crystallinity of approximately 36%. Subsequent heating at 10 °C/min gives a double peaked melting curve, with peak values just above 245 °C and just above 250 °C. Heating at 100 °C/min changes this double peak into a single peak, at approximately 245 °C. Apparently, reorganization (probably by recrystallization) is successfully prevented by a higher heating rate. Cooling at 100 °C/min shifts the crystallization peak value from 200 °C to a much lower value of 162 °C, while the crystallinity is also lowered to the much lower value of approximately 10% compared to 36%. Heating at 10 and 100 °C/min shows cold crystallization in both cases. This illustrates the metastable character of the crystals formed, which is due to the relatively high cooling rate. So, obviously, even the heating rate of 100 °C/min, after cooling at 100 °C/min, is not high enough to avoid cold crystallization. Because

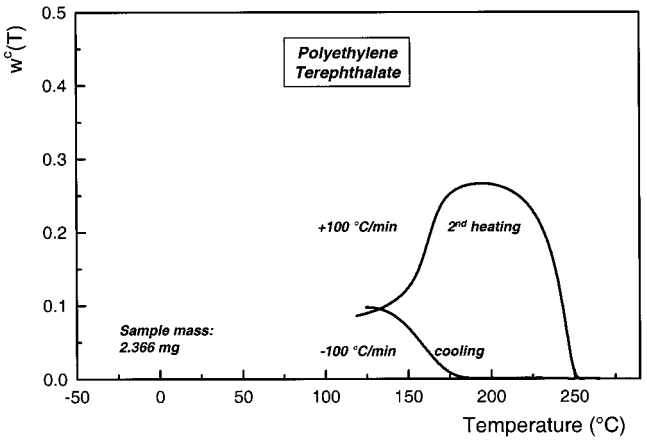

Figure 12. Enthalpy-based mass fraction crystallinities for a polyethylene terephthalate sample (2.366 mg): crystallization (to approximately 10% crystallinity) during cooling at 100 °C/min; cold crystallization (to approximately 27% crystallinity) and melting during subsequent heating at 100 °C/min. Purge gas: helium (10)/neon (90).

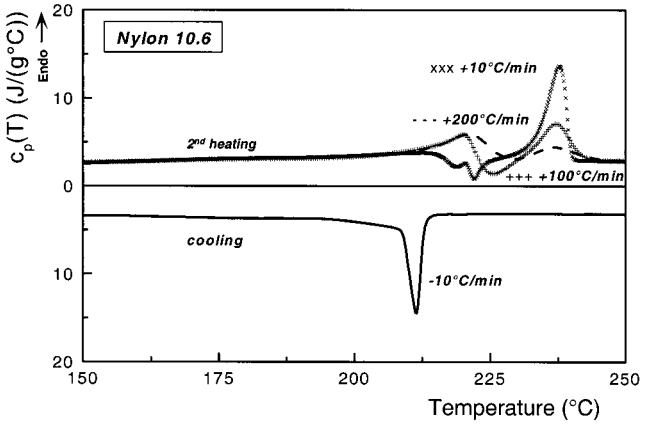

Figure 13. Various second heating curves, at scan rates of 10, 100, and 200 °C/min, after cooling at 10 °C/min for a Nylon 10.6 sample. The extensive reorganization that occurs during heating at low scan rates is increasingly hindered as the scan rate increases.

of this cold crystallization, the crystallinity increases during heating from 10% to a maximum of approximately 27% (which is still lower than the 36% obtained in cooling at 10 °C/min) before decreasing to zero as the sample melts completely; see Figure 12. This example convincingly shows that even at the extreme conditions applied—high scan rates and a low sample mass of milligram level—quantitative measurements can be performed, because instrumental drift is virtually absent. Thus, *heat capacities, enthalpies, crystallinities, baseline, and excess heat capacities*[45] can be determined at high scan rates.

Another example of the great potential of HPer DSC in studying and influencing metastability is the melting behavior of a Nylon 10.6 sample;[62] see Figure 13, after cooling at 10 °C/min.

During the 10 °C/min cooling scan, the sample crystallizes at a maximum rate around 210 °C. The heating rate that is subsequently chosen has a major influence on the shape of the heating curve. Heating at 10 °C/min initially shows a relatively small endothermal effect, which, in the temperature region just above the onset of crystallization, is followed by a clearly distinguishable but likewise small exothermal effect. The melting and recrystallization processes probably partially overlap, which would explain the relatively weak net signal. Further heating produces a melting peak around 237 °C. Even in a heating run at 100 °C/min, there is still an exothermal effect. The first melting peak is now more distinct and has its maximum around 220 °C. It seems plausible to relate this peak to the crystallization peak around 210 °C. The second peak once again has a maximum at 237 °C and is substantially smaller than the peak obtained in the heating run at 10 °C/min. This effect is even more pronounced in the case of heating at 200 °C/min: the second peak once again lies around 237 °C, and no exothermal effect is visible. All this points to a substantial degree of reorganization during heating, probably by recrystallization, as is also evidenced by the constant net total area of 47.5 ± 1.0 J/g under the heating curves obtained at 10, 100, and 200 °C/min. Also, it is conceivable that there are transitions between the various crystal polymorphs. An X-ray study has been initiated to investigate this.[62] Another conclusion from the above findings is that apparently an even higher heating rate will be needed to prevent reorganization altogether (resulting in the complete disappearance of the second peak).

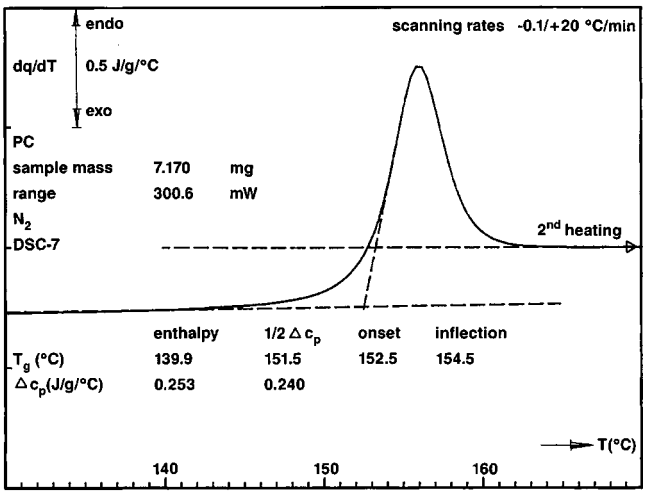

Figure 14. Second heating curve of a polycarbonate at 20 °C/min after cooling at 0.1 °C/min. Some "characteristic temperatures" that mark the glass transition: the "inflection point" ; the "onset" ; "$^1/_2\Delta c_p$"; the thermodynamic "enthalpy-based" T_g, or fictive, temperature.

Finally, an entirely different field of application of HPer DSC will be discussed now, namely the study of vitrification and devitrification as a function of the cooling and heating rate.[18] This application, too, involves the use of widely different scan rates and enables the curves to be evaluated in quantitative terms.

Figure 14 shows a heating curve (20 °C/min) for a polycarbonate previously cooled at 0.1 °C/min.[29] Using commercially available software packages, it is possible to determine "characteristic temperatures" of a glass transition curve, like the ones shown in Figure 14: an "onset" temperature; the temperature at which half of the total c_p jump (moving from below the glass transition temperature to above this temperature) can be determined, referred to as "$^1/_2\Delta c_p$"; the temperature of inflection (the temperature corresponding to the maximum in the first derivative of the DSC curves), etc. The aforementioned methods for determining the glass transition serve to chart the various aspects of the curve shape as a function of the cooling and heating rates. Some software packages additionally offer the possibil-

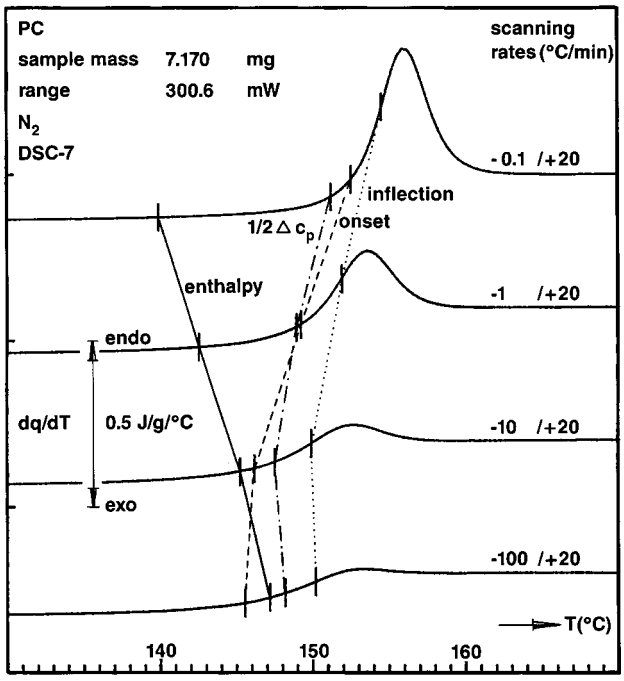

Figure 15. Second heating curves at 20 °C/min of a polycarbonate, after cooling at various rates: 0.1, 1, 10, and 100 °C/min. Locations of some "characteristic temperatures" that mark the glass transition and the thermodynamic "enthalpy-based" T_g as in the preceding figure.

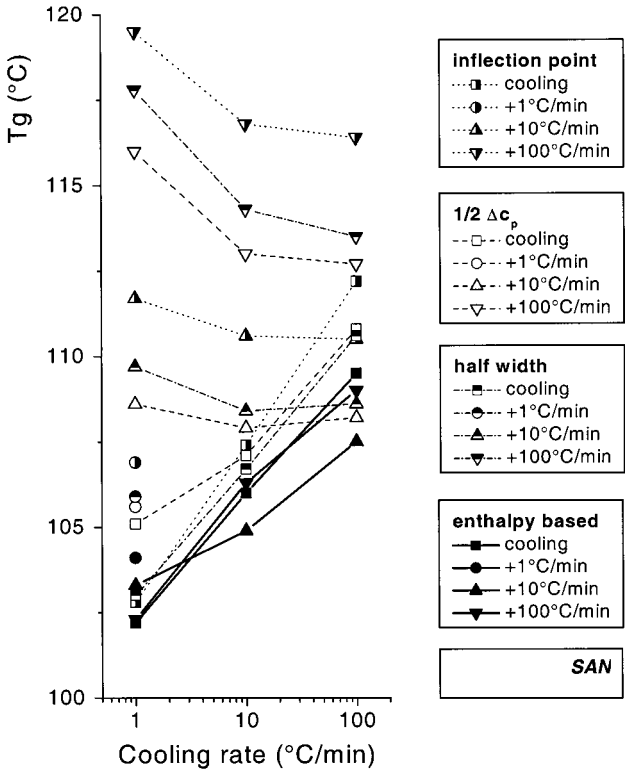

Figure 16. Some "characteristic temperatures" that mark the glass transition of a styrene acrylonitrile (SAN; 27% of AN) copolymer: the "inflection point"; "$^1/_2\Delta c_p$"; the "half-width"; the thermodynamic "enthalpy based" T_g, or fictive, temperature, as determined at different heating rates (1, 10, and 100 °C/min) after cooling at different rates (also 1, 10, and 100 °C/min).

ity of determining the "enthalpy-based" T_g, or fictive temperature, based on the "enthalpy method": the enthalpy curves before and after the transition are fitted using a second-order polynomial and a least-squares method (assuming the DSC curves to be linear in the regions mentioned, which is a good approximation, at least above the glass transition region). The intersection of these regressions is taken as a value for the T_g, which is why the glass transition temperature thus determined is also named the "isoenthalpic" T_g. This temperature alone determines the "intrinsic" glass transition temperature of the sample which is realized during cooling and which would have been measured by a DSC instrument if the cooling curves had been recorded. Obviously, this is not always possible, either because the cooling rate is too high to be imitated in a DSC instrument, as is the case with several processing methods, or because one has to measure the sample "as received" without knowing its thermal history. This glass transition temperature realized during cooling is of course not affected by heating in the DSC instrument. On the other hand, the way the sample takes up enthalpy—which well-known and extensively studied phenomenon is called "enthalpy recovery"—as reflected in the shape of the heating curve as a function of temperature, is strongly influenced by the heating rate, and by the sample history.[18] For example, see Figure 15, where the "inflection point" illustrates that when the heating rate is faster than the cooling rate the change in heat-flow rate in the heating curve occurs at higher temperatures and is followed by a peak in the curve (the temperature at which this peak occurs might be added to the list of characteristic temperatures). This figure shows heating curves (20 °C/min) for a polycarbonate previously cooled at different rates, ranging from 0.1 to 100 °C/min. Using the enthalpy method, it is possible to determine the glass transition temperature—reflecting a frozen-in and metastable state—and thus gain insight into the thermal history regardless of the way the sample is heated. The method is described in detail in ref 18. The result is shown in both Figures 14 and 15. For thermodynamic reasons, it is to be expected that the glass transition temperature increases with increasing cooling rate, and this trend is reflected only in the fictive temperature. All other characteristic temperatures show the opposite (i.e., wrong) trend: they suggest that T_g decreases as the cooling rate increases! So, if these temperatures are used as a basis for determining the glass transition temperature during cooling, they lead to wrong conclusions, as a result of which a research project may be steered in the wrong direction. It is obvious that the enthalpy method should be used, if only to enable comparisons with results obtained by other techniques.

In the same way, Figure 16 shows the influence of the cooling rate (1, 10, and 100 °C/min) and the heating rate (also 1, 10, and 100 °C/min) for a styrene acrylonitrile (SAN) copolymer. Again, Figure 16 shows the results of monitoring the glass transition via "characteristic temperatures", using slightly different definitions, because now commercial PerkinElmer software was used: the "inflection point", "$^1/_2\Delta c_p$", the "half-width" (the temperature belonging to the point on the curve that is halfway between the onset and end points, as defined and determined by the PerkinElmer software), and the "enthalpy-based" one.

Using the HPer DSC procedure, the sample masses were now adjusted to suit the various scan rates. Specific values used were 50.754 mg for a scan rate of 1 °C/min, 9.813 mg for a rate of 10 °C/min, and 0.792 mg for a rate of +100 °C/min.

Enthalpy recovery is again clearly visible in Figure 16, for example at a constant cooling rate of 1 °C/min. When the heating rate is increased from 1 via 10 to 100 °C/min, it is seen that the temperature defined by the "inflection point" increases by about 12 deg. Relating such a change in the heat-flow rate curve to processing conditions or properties can be important in industrial practice.

The 12-deg upward shift of the "inflection point" that is observed when the heating rate is increased from 1 to 100 °C/min after cooling at 1 °C/min is also found for the other characteristic temperatures: the "$^1/_2\Delta c_p$" temperature and the "half-width" temperature.

However, this does not imply that T_g increases by 12 deg, because that would make the glass transition temperature dependent on the ratio of the heating rate and the cooling rate or, in the case of a fixed cooling rate, on the heating rate alone. This would be absurd from a thermodynamic point of view; after all, the glass transition temperature is determined by the cooling rate, and the method for determining the "enthalpy-based" T_g is the only method that is in line with this thermodynamic approach. It is assumed that—for the conditions chosen—enthalpy relaxation during the isothermal stays and during heating, which would result in a change in glass transition temperature, does not occur.

The fact that T_g after cooling at 1 °C/min is not influenced by the heating rate (which in these experiments was varied from 1 via 10 to 100 °C/min) is clearly illustrated by the values of the enthalpy-based T_g at these different heating rates: these values are virtually constant (as was to be expected) at 103 ± 1 °C. They are in good agreement with the T_g measured in cooling at 1 °C/min: 102 °C; see Figure 16.

The difference between the various characteristic temperatures can be quite large. For example, if the "inflection point" temperature and "enthalpy-based" T_g after cooling at 1 °C/min and heating at 100 °C/min are compared, a difference of 17 °C is seen. The figure further shows that the trends are totally different. The "inflection point" temperature decreases with increasing cooling rate (and constant heating rate), while the "enthalpy-based" T_g shows the reverse trend. The latter is the correct trend; it is the trend one would expect on the basis of thermodynamic considerations. Its correctness is confirmed by measurements of the characteristic temperatures in cooling: all of these temperatures increase as the cooling rate increases. The "enthalpy-based" T_g values determined in cooling at 1, 10, and 100 °C/min agree very well with the "enthalpy-based" T_g values determined in a subsequent heating scan at 100 °C/min. The change in the "enthalpy-based" T_g values as a function of the cooling rate amounts to 3.5 °C/(decade in cooling rate). Heating at 10 °C/min also yields an acceptable result: agreement within 2 deg, possibly a slightly different slope, and of course, the correct trend. Clearly, HPer DSC is very suitable for such studies, the more so as it enables the scan rate to be varied to an even greater extent than shown here, using submilligram sample masses.

4. Outlook

Up to now, controlled constant rates as high as hundreds of °C/min have been realized. Of course, there is still room for improvement. After all, the authors obtained the results described here by setting up effective procedures and by making relatively simple modifications to an existing, commercially available calorimeter. It would be enlightening to hear from the manufacturer why the results obtained are so good, and what hardware and software configurations have been used to achieve such a performance. It should be noted, though, that this performance cannot be achieved with the earlier types of DSC (No. 2 and No. 7) and not even with all versions of the Pyris instrument. It goes without saying that modeling[63] such an instrument in terms of heat flows is no simple exercise and may even be impossible without additional, detailed information. Obviously, the manufacturer has access to hardware and software know-how that is not available to the authors and can use this know-how to optimize the equipment so as to further expand the range of possibilities in the direction indicated. This will probably enable even higher (constant) rates to be achieved in the temperature ranges that are important for polymers and pharmaceuticals. If the calorimeter design is modified in a targeted way, a substantial further expansion of the range of possibilities may even be feasible, until the heat exchange between the sample and its surroundings becomes a limiting condition. In our opinion, the poor thermal conductivity of a polymer sample is not the biggest problem, because the sample mass can be chosen considerably lower; see the experiment with ultrahigh molecular weight polyethylene on a microgram scale. The use of a highly conductive sample packaging material (in this case aluminum foil), which completely envelops the sample, will then result in optimum heat transfer between the sample and its surroundings.

Further, drastic improvements will be possible only if the design of the calorimeter is thoroughly renewed. Miniaturization will be the key to success.[25,64,65] "Calorimetry-on-the-chip" with the aid of nanotechnology should lead to a major improvement (i.e., increase) in scan rates.

It is hardly possible to overemphasize the importance of extremely high cooling rates, not only for imitating important processing methods but also for suppressing or even preventing crystallization in cooling (keeping a sample in the amorphous state until the glass transition is reached). In addition, extremely high heating rates are important for reducing or even eliminating reorganization during heating. For both scientific and industrial research, the sky is the limit as far as scan rates are concerned.

Whether the development sketched above—which is of paramount importance for both scientific and industrial research—will become a reality is hard to predict at this moment. In any case, a compromise will have to be sought between the ideal situation sketched above and the technical feasibility. Commercial realization will depend on the potential market, i.e., the demand from potential users.

5. Conclusions

HPer DSC—High Performance DSC—is excellently suited for studying the kinetics and metastability of polymer systems, because it is capable of applying very high, controlled and constant scan rates (hundreds of degree per minute) and combinations thereof both in cooling and in heating: it is also a *high rate DSC*.

(De)vitrification, crystallization, and solid−solid-phase transitions can be measured under much more

realistic conditions, as occurring in practice during fast-cooling processes; moreover, these processes can be understood much better because reorganization phenomena during heating like cold crystallization, recrystallization, etc.—which obscure the interpretation of melting and solid−solid-phase transitions—can be studied, influenced, and in some cases, even avoided.

As instrumental drift is minimal during the very short times of measurement, quantitative results can be obtained. Thus, even heats of transition and heat capacities can be established at the extreme rates applied.

Sample masses ranging from approximately 1 mg down to a few micrograms can be utilized. This will facilitate research on heterogeneities, additives, dispersed substances, nanoparticles, fractions, etc. present in very low concentrations or available in minute amounts. Coatings, thin films, and multilayered structures can also be measured at high sensitivity.

The extremely high scan rates applied in HPer DSC enable the measurement time to be drastically reduced. This is an advantage in high throughput research—for example in combinatorial chemistry. However, quality control (QC), measurement of specifications of samples and products, etc. will also be fruitful areas of application: HPer DSC is also a *high throughput DSC*.

Although the application of HPer DSC in polymer research is obvious, the new method/technique will be of use for measurements on all kinds of substances, materials and products thereof that consist of high and/or low molar mass molecules.

Thus, the capabilities of HPer DSC, as mentioned, will be of advantage in different fields, including material science, the life sciences, pharmaceutics, solid-state physics, etc. and thus provide analytical support to (bio)-chemistry and physics research.

Finally, the development presented here should be regarded as a first step: via "calorimetry-on-the-chip" with the aid of nanotechnology it should be possible to reach much higher scan rates.

References and Notes

(1) Wunderlich, B. *Macromolecular Physics*; Academic Press: New York, 1976; Vol. 2 (Crystal Nucleation, Growth, Annealing).
(2) Wunderlich, B. *Macromolecular Physics*; Academic Press: New York, 1980; Vol. 3 (Crystal Melting).
(3) Keller, A. *Macromol. Symp.* **1995**, *98*, 1.
(4) Mathot, V. B. F.; Scherrenberg, R. L.; Pijpers; T. F. J. *Polymer* **1998**, *39*, 4541.
(5) Filonov, A. M.; Novikova, O. S.; Tsekhanskaya, Yu. V. *Zh. Fiz. Khim.* **1974**, *48*, 1597.
(6) Brucato, V.; Crippa, G.; Piccarolo, S.; Titomanlio, G. *Polym. Eng. Sci.* **1991**, *31*, 1411.
(7) Piccarolo, S.; Saiu, M.; Brucato, V.; Titomanlio, G. *J. Appl. Polym. Sci.* **1992**, *46*, 625.
(8) Ratasjski, E.; Janeschitz-Kriegl, H. *Colloid Polym. Sci.* **1996**, *274*, 938.
(9) Janeschitz-Kriegl, H.; Ratasjski, E.; Wippel, H. *Colloid Polym. Sci.* **1996**, *277*, 217.
(10) Wunderlich, B.; et al. *J. Polym. Sci., Part A-2* **1969**, *7*, 2043, 2051, 2061, 2073, 2091, 2099.
(11) Bassett, D. C.; Turner, B. *Nature (Phys. Sci.)* **1972**, *240*, 146.
(12) Rastogi, S.; Newman, M.; Keller, A. *J. Polym. Sci., Part B: Polym. Phys.* **1993**, *31*, 125.
(13) Vanden Eynde, S.; Mathot, V. B. F.; Höhne, G. W. H.; Schawe, J. W. K.; Reynaers, H. *Polymer* **2000**, *41*, 3411.
(14) Vanden Eynde, S.; Rastogi, S.; Mathot V. B. F.; Reynaers, H. *Macromolecules* **2000**, *33*, 9696.
(15) Eder, G.; Janeschitz-Kriegl, H. Crystallization. In *Processing of Polymers*; Meijer, H. E. H., Ed.; Material Science and Technology 18; Cahn, R. W., Haasen, P., Kramer, E. J., Vol. Eds.; VCH Verlagsgesellschaft mbH: Weinheim, Germany, 1997; Chapter 5, pp 296−344.
(16) Zuidema, H. Thesis Flow Induced Crystallization of Polymers, Application to Injection Moulding. Technische Universiteit Eindhoven, Eindhoven, The Netherlands, 2000; ISBN 90-386-3021-2; 126 pages.
(17) Hsiung, C. M.; Cakmak, M. *Polym. Eng. Sci.* **1991**, *31*, 1372.
(18) Richardson, M. J. In *Calorimetry and Thermal Analysis of Polymers*; Mathot, V. B. F., Ed.; Hanser Publishers: Munich, Germany, Vienna, and New York, 1994; Chapter 6 (The Glass Transition Region), p 169.
(19) Mathot, V. B. F. In *Calorimetry and Thermal Analysis of Polymers*; Mathot, V. B. F., Ed.; Hanser Publishers: Munich, Germany, Vienna, and New York, 1994; Chapter 9 (The Crystallization and Melting Region), p 231.
(20) Hager, N. E., Jr. *Rev. Sci. Instrum.* **1964**, *35*, 618.
(21) Hellmuth, E.; Wunderlich, B. *J. Appl. Phys.* **1965**, *36*, 3039.
(22) Hager, N. E., Jr. *Rev. Sci. Instrum.* **1972**, *43*, 1116.
(23) Shlenskii, O. F.; Vishnevskii, G. E. *Dokl. Akad. Nauk SSSR* **1984**, *279*, 105.
(24) Fröchte, B.; Khan, Y.; Kneller, E. *Rev. Sci. Instrum.* **1990**, *61*, 1954.
(25) Lai, S. L.; Ramanath, G.; Allen, L. H.; Infante, P.; Ma, Z. *Appl. Phys. Lett.* **1995**, *67*, 1229.
(26) Domszy, R. *Proceedings Metallocenes '96*; Düsseldorf, Germany, 1996; p 251.
(27) Lai, S. L.; Ramanath, G.; Allen, L. H. *Appl. Phys. Lett.* **1997**, *70*, 43.
(28) Blaine, R. L.; Slough, C. G.; Price, D. M. In *Proceedings of the NATAS (North American Thermal Analysis Society) 28th Annual Conference on Thermal Analysis and Applications, October 4−6, Orlando, FL*; Kociba, K. J., Ed.; 2000; p 883.
(29) Mathot, V. B. F. *Thermochim. Acta* **2000**, *355*, 1.
(30) Mathot, V. B. F. *J. Therm. Anal. Calorim.* **2001**, *64*, 15.
(31) Kwan, A. T.; Efremov, M. Yu.; Olson, E. A.; Schiettekatte, F.; Zhang, M.; Geil, P. H.; Allen, L. H. *J. Polym. Sci.* **2001**, *39*, 1237.
(32) Goderis, B.; Peeters, M.; Mathot, V. B. F.; Koch, M. H. J.; Bras, W.; Ryan, A. J.; Reynaers, H. *J. Polym. Sci., Part B: Polym. Phys.* **2000**, *38*, 1975.
(33) Pijpers, Thijs, F. J.; Mathot, Vincent, B. F.; Goderis, Bart; van der Vegte, Eric. In *Proceedings of the NATAS (North American Thermal Analysis Society) 28th Annual Conference on Thermal Analysis and Applications, October 4−6, Orlando, FL*; Kociba, K. J., Ed.; 2000; pp 32−37.
(34) Pijpers, T.; van der Vegte, E.; Mathot, V.; Cassel, B. In *Proceedings of the NATAS (North American Thermal Analysis Society) 28th Annual Conference on Thermal Analysis and Applications, October 4−6, Orlando, FL*; Kociba, K. J. Ed.; 2000; pp 32−37.
(35) Gorbrecht, H.; Hamann, K.; Willers, G. *J. Phys. E: Sci. Instrum.* **1971**, *4*, 21.
(36) Reading, M.; Elliot, D.; Hill, V. L. *J. Therm. Anal.* **1993**, *40*, 949.
(37) Special issue: Thermal Analysis and Calorimetry in Polymer Physics. Mathot V. B. F., Ed. *Thermochim. Acta* **1994**, *238*.
(38) Special issue: Temperature Modulated Calorimetry. Schick, C., Höhne, G. W. H.; Eds. *Thermochim. Acta* **1997**, *304/305*.
(39) Special issue: Temperature Modulated DSC; Judovits, L. H., Menczel J. D., Eds.; *J. Therm. Anal.* **1998**, *54*.
(40) Special issue: Lähnwitz Seminar on Temperature Modulated DSC 1998. Schick, C., Höhne G. W. H., Eds.; *Thermochim. Acta* **1999**, *330*.
(41) Wunderlich, B. *Thermochim. Acta* **2000**, *355*, 43.
(42) Goderis, B.; Reynaers, H.; Scherrenberg, R.; Mathot, V. B. F.; Koch, M. H. J. *Macromolecules* **2001**, *34*, 1779.
(43) Mraw, S. C.; Naas, D. F. *J. Chem. Thermodyn.* **1979**, *11*, 567.
(44) Fransson, Å.; Bäckström, G. *Int. J. Thermophys.* **1985**, *6*, 165.
(45) Mathot, V. B. F. In *Calorimetry and Thermal Analysis of Polymers*; Mathot, V. B. F., Ed.; Hanser Publishers: Munich, Germany, Vienna, and New York, 1994; Chapter 5 (Thermal Characterization of States of Matter), p 105.
(46) Richardson, M. J. In *Calorimetry and Thermal Analysis of Polymers*; Mathot, V. B. F., Ed.; Hanser Publishers: Munich, Germany, Vienna, and New York, 1994; Chapter 4 (DSC on Polymers: Experimental Conditions), p 91.
(47) Wunderlich, B.; Boller, A.; Okazaki, I.; Ishikiriyama, K.; Chen, W.; Pyda, M.; Pak, J.; Moon, I.; Androsch, R. *Thermochim. Acta* **1999**, *330*, 21.
(48) Janeschitz-Kriegl, H.; Wippel, H.; Paulik, Ch.; Eder, G. *Colloid Polym. Sci.* **1993**, *271*, 1107.

(49) Wu, C. H.; Eder, G.; Janeschitz-Kriegl, H. *Colloid Polym. Sci.* **1993**, *271*, 1116.
(50) Merzlyakov, M.; Schick, C. *Thermochim. Acta* **1999**, *330*, 65.
(51) Vonnegut, B. J. *J. Colloid Sci.* **1948**, *3*, 563.
(52) Cormia, R.; Prize, F. P.; Turnbull, D. *J. Chem. Phys.* **1962**, *37*, 1333.
(53) Koutsky, J.; Walton, A. G.; Baer, E. *J. Appl. Phys.* **1967**, *38*, 1832.
(54) Barham, P. J.; Jarvis, D. A.; Keller, A. *J. Polym. Sci., Polym. Phys.* **1982**, *20*, 1773.
(55) Frensch, H.; Harnischfeger, P.; Jungnickel, B. J. Multiphase Polymers: Blends and Ionomers. *ACS Symp. Ser.* **1989**, *395*, 101.
(56) Everaert, V.; Groeninckx, G.; Aerts, L. *Polymer* **2000**, *41*, 1409.
(57) Billon, N.; Magnet, C.; Haudin, J. M.; Lefebvre, D. *Colloid Polym. Sci.* **1994**, *272*, 633.
(58) Wunderlich, B.; Mehta, A. *J. Polym. Sci., Part B: Polym. Phys.* **1974**, *12*, 255.
(59) Todoki, M.; Kawaguchi, T. *Rep. Prog. Polym. Phys. Jpn.* **1979**, *22*, 241.
(60) Todoki, M. *Thermochim. Acta* **1985**, *93*, 147.
(61) ATHAS data bank. For a description see: Wunderlich, B. *Pure Appl. Chem.* **1995**, *67*, 1019. Detailed information may also be found on the Internet: http://web.utk.edu/~athas.
(62) Goderis, B.; Koning, C. To be published.
(63) Höhne, G. W. H. In *Calorimetry and Thermal Analysis of Polymers*; Mathot, V. B. F., Ed.; Hanser Publishers: Munich, Germany, Vienna, and New York, 1994; Chapter 3 (Fundamentals of Differential Scanning Calorimetry and Differential Thermal Analysis) p 47.
(64) Kitahara, T.; Nakai, K. *Int. J. Microcircuits Electron. Packag.* **1997**, *20*, 274.
(65) Nakagawa, Y.; Schäfer, A.; Güntherodt, H.-J. *Appl. Phys. Lett.* **1998**, *73*, 2296.

MA011122U